ISSN 1063-7745, Crystallography Reports, 2023, Vol. 68, No. 1, pp. 104–109. © Pleiades Publishing, Inc., 2023.
Russian Text © The Author(s), 2023, published in Kristallografiya, 2023, Vol. 68, No. 1, pp. 94–99.

SURFACE
AND THIN FILMS

X-ray Reflectometry of Thin Films Formed during Phase Separation of Organic Solutions of Aliphatic Polyethers in Water

V. E. Asadchikov[a,*], Y. O. Volkov[a], B. S. Roshchin[a], A. D. Nuzhdin[a], E. R. Chernavskaya[b], A. M. Tikhonov[c], A. V. Mironov[a], A. O. Mariyanac[a], and V. K. Popov[a]

[a] *Shubnikov Institute of Crystallography, Federal Scientific Research Centre "Crystallography and Photonics," Russian Academy of Sciences, Moscow, 119333 Russia*

[b] *National Research Nuclear University MEPhI (Moscow Engineering Physics Institute), Moscow, 115409 Russia*

[c] *Kapitza Institute for Physical Problems, Russian Academy of Sciences, Moscow, 119334 Russia*

**e-mail: asad@crys.ras.ru*

Received August 29, 2022; revised August 29, 2022; accepted August 31, 2022

Abstract—The possibilities of X-ray reflectometry for studying the structure of planar liquid-phase membranes are demonstrated by the example of polyester films formed on the surface of deionized water from solutions of polylactoglycolide (PLG) in chloroform and tetraglycol (TG). It is found that the use of solutions with PLG concentrations ranging from 1 to 4 wt % or above 6 wt % leads to a proportional increase in the density of these films with preservation of their structure and thickness up to 25 Å. At a PLG concentration close to 5 wt % the PLG/TG system transits to an unstable state, characterized by intense penetration of PLG aliphatic chains into the water substrate bulk to a depth up to 100 Å.

DOI: 10.1134/S1063774523010029

INTRODUCTION

Biocompatible polymers, which can undergo controlled biodegradation or bioresorption when contacting with living organism tissues, are widely used to develop and design diverse products for medicine and biology, as well as to solve various problems of tissue engineering and regenerative medicine [1]. One of these problems is the creation, study, and application of personalized tissue-engineered constructs (TECs) based on bioresorbable matrices of a certain architectonics, which play the role of a three-dimensional scaffold for colonization, differentiation, and proliferation of donor or autologous cells of certain types [2]. A fundamental requirement for matrices is the presence of a system of communicating pores of certain sizes (generally from 100 to 700 μm) in their structure, which should provide the delivery of nutrients and oxygen to living cells and remove toxic products of their metabolism [3].

There are many different methods and technologies used to produce bioresorbable polymer matrices (mainly based on polymers of the homologous series of aliphatic polyesters: polylactides, polyglycolides, and their copolymers [4, 5]) for TECs of desired shape and structure [6]. Primarily, these are leaching [7], phase separation at cryoprocessing [8, 9], supercritical fluid foaming [10], and electrospinning [9, 11]. One of widespread methods of forming polymer membranes [12] and films is the phase separation at the contact boundary between the polymer solution and precipitant [13, 14]. Depending on the physicochemical properties of a particular system and the conditions for forming a polymer phase in it, one can obtain a variety of different macrostructures of final material: from an isotropic monolith to microstructures of gradient porosity or a combination of them. The isotropy of bulk phases is violated in these heterogeneous systems, which may lead, for example, to directed two-dimensional crystallization [15, 16] or formation of fingerlike pores [17].

Apparently, one of the most promising approaches to the development and fabrication of bioresorbable matrices for TECs of specified and, most importantly, reproducible architectonics is the use of additive manufacturing technologies (AMTs) or 3D printing [18]. Among the numerous processes AMTs are based on, in the context of this study, we should highlight the proposed and previously developed method of antisolvent 3D printing [17], based on the formation of a polyester matrix at the phase separation of a polymer solution in an organic solvent during extraction of the latter in the surrounding water medium. In this case, the microstructure of the manufactured matrix will be determined by the kinetics of the phase separation and mass transfer processes, and its macrostructure and shape will be set by the preselected three-dimensional digital model.

One of the systems that were used and investigated previously for antisolvent printing of matrices for TECs is the solution of the biologically compatible copolymer of lactic and glycolic acids—polylactoglycolide (PLG) [19]—in tetraglycol (TG) [20], which forms a highly porous solid structure upon contact with aqueous media (antisolvents). Tetraglycol is a nontoxic solvent for a number of different hydrophobic polyethers, and is indefinitely miscible with water. Due to this, TG can be efficiently extracted from polymer solutions with controlled solidification of materials dissolved in them. A significant advantage of the PLG/TG/water system is that it has low toxicity and does not require elevated temperatures in the processes under study, which is highly important for biomedicine. According to [19], antisolvent PLG precipitation makes it possible to obtain structures of different types on the scale from 1 to 100 μm, depending on the phase-separation conditions. At the same time, the formation of a primary subnanometer polymer layer on the contact boundary between the polymer solution and precipitant (water), which affects to a great extent subsequent mass transfer processes; concentration distribution dynamics; and, as a consequence, the type and properties of the microstructure formed, was not considered.

In this paper, we report the results of experimental study and simulation of the structure of polymer layers formed during phase separation of PLG solutions in chloroform and TG at their contact boundary with distilled water. Data on the distribution of the components of the PLG/TG/water ternary system at the interface were obtained with the use of X-ray reflectometry [21], which is based on the phenomenon of total external reflection of X-rays from the interface in the grazing incidence geometry. Since this method is nondestructive, it is widely applied to study the structure of thin-film planar objects (including membrane layers) on the molecular scale, both during their synthesis and modification [22]. The model-independent algorithm of structure reconstruction, applied in this study, makes it possible to reconstruct the distribution of density in the direction perpendicular to the surface, with a nanoscale resolution, requiring no additional information about the crystalline structure of the object studied [23]. For this reason this method is well suited, in particular, to investigations of liquid layers on the liquid substrate surface.

Note that, in view of the low contrast of liquid-phase media in the X-ray range, as well as the influence of temperature and vibrations on the roughness of the interface between fluid media, these reflectometric experiments are usually performed on synchrotron sources. However, as was shown in this study, a combination of measurements on specialized laboratory sources with application of model-independent reconstruction algorithms makes it possible to extract structural information of comparable quality.

MATERIALS AND METHODS

To study the structure of aliphatic polyester films, PLGA 7502 (Purasorb Biochem BV) with a characteristic viscosity of 0.2 dL/g and a lactide : glycolide ratio of 75 : 25 was used as a model compound. Two series of PLG solutions in chloroform and/or TG with PLG mass concentrations of 1, 2, 3, 4, 5, 6, 7, and 10 wt % were prepared initially. The solutions of the first series were obtained by the method of successive dilutions of the initial 10% solution. In the samples of the second series the PLG amount was measured separately for each solution.

Solutions were prepared using weights of initial components on an analytical laboratory balance. Stirring was performed with a magnetic agitator at 40°C in a glass vessel equipped with a ground-in lid to exclude penetration of atmospheric moisture.

The experimental samples were formed on the water surface in a Teflon dish 100 mm in diameter, mounted in a sealed one-step thermostat [24]. A fixed volume (10 and 20 mL) of PLG solution in TG was deposited on the substrate surface by the drop method using a calibrated Hamilton syringe, with subsequent spreading over the meniscus surface for 15 min. The prepared samples were kept in a thermostat at a fixed temperature: $T = 295$ K.

Measurements were performed on a general-purpose laboratory diffractometer with a mobile source–detector system (Federal Scientific Research Centre "Crystallography and Photonics" of the Russian Academy of Sciences). The diffractometer design was described in detail in [25]. A wide-focus (12×2 mm^2) X-ray copper-anode tube was used as a radiation source. Probe radiation was formed using a single-reflection monochromator crystal Si(111), tuned to the copper $K_{\alpha 1}$ line (photon energy $E \approx 8048$ eV, wavelength $\lambda = 1.5405 \pm 0.0001$ Å), and an evacuated three-slit collimation system, which provided a linear beam width (intensity distribution in the mirror-reflection plane) $d \approx 0.55$ mm and a divergence of ~1.5′ at a total intensity of 3×10^6 counts/s. Signal detection was performed using a Radicon SCSD-4 scintillation detector (noise level 0.1 counts/s). Thus, the measurement range relative to decrease in signal intensity I_{max}/I_{min} was 7 to 8 orders of magnitude, which is comparable with measurements on second-generation synchrotron sources [26].

Under specular reflection conditions the X-ray scattering vector has a single component, directed normally to the interface: $q_z = |k_{in} - k_{sc}| = (4\pi/\lambda)\sin\alpha$, where α is the grazing angle and k_{in} and k_{sc} are, respectively, the wave vectors of the incident beam and the beam scattered towards the observation point. The critical angle of total external reflection from the surface, $\alpha_c = \lambda\sqrt{r_0\rho_w/\pi}$ (where $r_0 = 2.814 \times 10^{-5}$ Å is the classical electron radius) is determined by the volume electron density ρ_w in the sample bulk. Note that

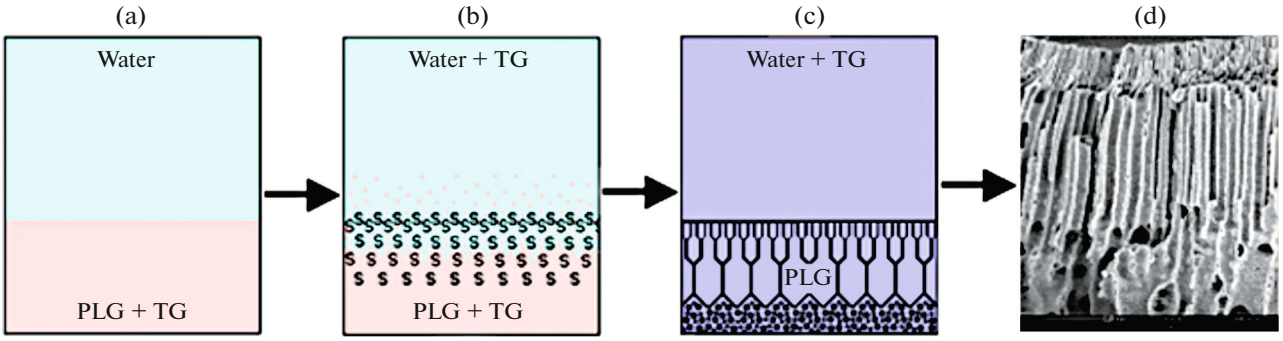

Fig. 1. (a–c) Evolution of the macrostructure in the ternary system polylactoglycolide–tetraglycol–water and (d) the newly formed structure of polymer phase.

$\rho_w = 0.333$ Å^{-1} for deionized water under normal conditions, which corresponds to the critical angle $\alpha_c \approx 0.153°$ in the experiment.

In turn, the angular dependence of specular reflectance has the form $R(q_z) = R_F(q_z)|\Phi(q_z)|^2$, where R_F is the reflectance from the ideal air–material interface and $\Phi(q) = \frac{1}{\rho_w}\int_{-\infty}^{+\infty}\left\langle\frac{d\rho(z)}{dz}\right\rangle e^{iqz}dz$ is the structure factor of distribution of electron density ρ inwards along the normal to the surface, averaged over the area of exposure.

To analyze the experimental curves of specular reflection $R(q_z)$ and reconstruct the distribution of electron density $\rho(z)$ from these curves, we applied the model-independent approach developed in [23, 27], which is based on extrapolation of the asymptotic component of reflectance R to large angles ($q_z > q_{max}$). In contrast to the classical approaches, which imply parameter optimization of a theoretical model of the desired object, the model-independent approach implements direct calculation of the distribution of volume electron density $\rho(z)$, without any a priori assumptions about the sample structure. The specific features of the approach, the problem of solution uniqueness, and the calculation algorithm were described in detail and discussed in [27].

RESULTS AND DISCUSSION

The formation of developed polymer structures during phase separation of PLG solutions in TG at their contact boundary with distilled water occurs in clearly pronounced stages. The first is the formation of a surface semipermeable layer from the saturated polymer solution: a gel layer. Figure 1 shows the schematic evolution of the polymer film (membrane) structure at the interface. On the whole, the structure is visualized well by the methods of optical and scanning electron microscopy [17]; an exception is the surface film of subnanometer thickness, which determines to a great extent the rate of mass-exchange processes between phases.

In contrast to the case of solutions in TG, the formation of the polymer phase from PLG solutions in chloroform occurs when the solvent is extracted into atmosphere (evaporates) without participation of aqueous phase in this process. Thus, there is barely any mass transfer through the interface between the polymer hydrophobic solution and water.

The results of studying the film of PLG solution in chloroform (20 μL) are presented in Fig. 2a. To control the film stability, additional measurements were performed 3 and 24 h after the sample preparation. The reflection curves contain periodic oscillations, which indicate the presence of a pronounced interface between the substrate and surface layer. The corresponding calculated density profiles are shown in Fig. 2b. One can see that PLG forms a surface film ~50 Å thick, which contains two pronounced sublayers of the same thickness (~25 Å) and density (~$1.22\rho_w$). The estimated value of the characteristic transition-layer thickness (roughness) σ at the polymer–substrate and polymer–air interfaces turned out to be 2.5 Å, which is also in agreement with the well-known roughness value of capillary waves on the water surface [28]. Thus, the film is presumably formed by a double folded layer of PLG molecules, oriented mainly in the surface plane, without penetration of polymer fragments into the substrate bulk.

The results of studying the films of PLG dissolved in the TG are shown in Fig. 3a for diluted solutions (20 μL) and in Fig. 3b for individual solutions (10 μL). The data obtained by measuring the surface of pure TG layer on deionized water (circles in Fig. 3a) served as reference ones. For both series of solutions the asymptotic falloff of the curves from the samples with concentrations of 5 and 10 wt % differs significantly from the others, which indicates a qualitative difference in their structures.

The calculated density profiles are presented in Fig. 4. The density of pure TG layer on water (Fig. 4a, lower curve) is close to that of the water substrate,

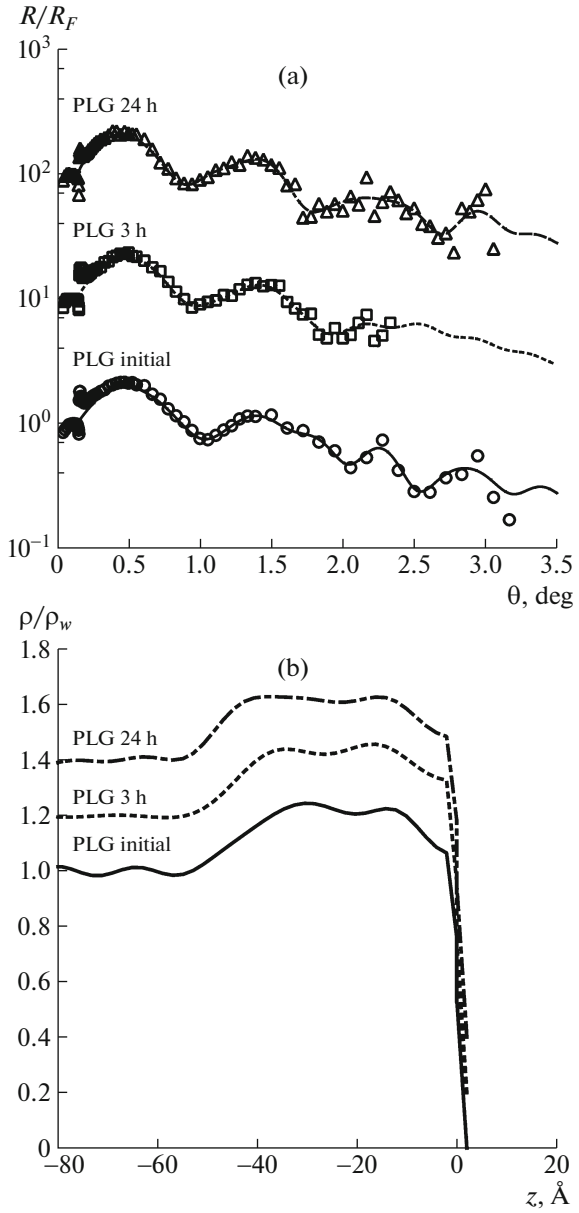

Fig. 2. (a) Moduli of the structure factor R/R_F and (b) the depth profiles of electron density ρ, normalized to the tabular water density $\rho_w = 0.333$ Å^{-3}, obtained for polylactoglycolide solutions in chloroform: (symbols) experimental data and (solid lines) calculation results.

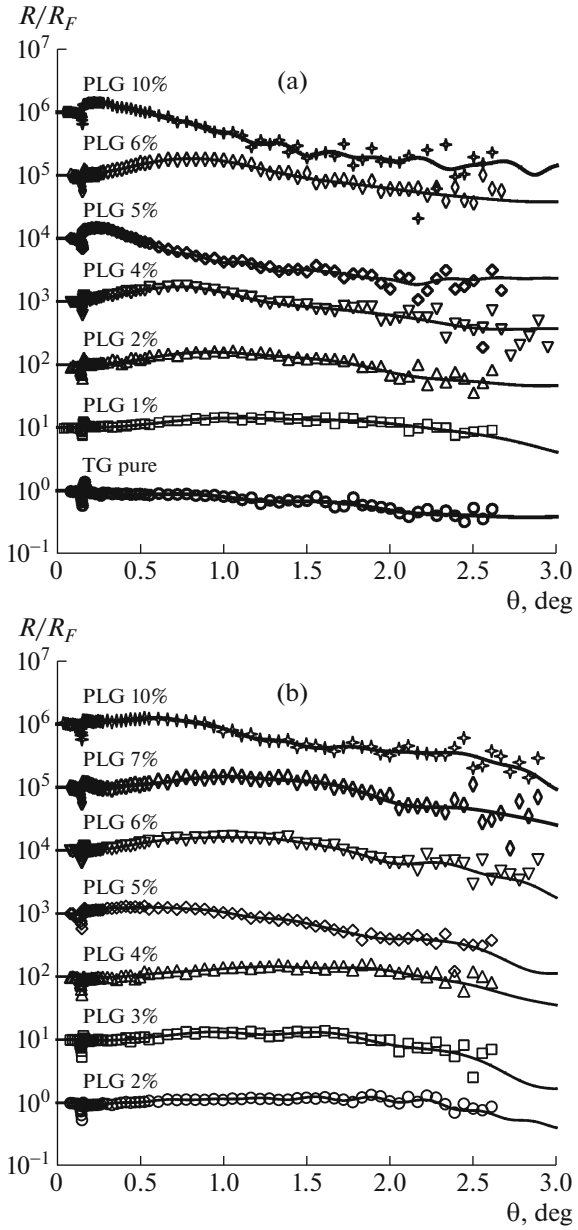

Fig. 3. Moduli of the structure factor R/R_F, obtained for polylactoglycolide solutions in tetraglycol, prepared (a) by the method of successive dilutions and (b) based on the weight ratio: (symbols) experimental data and (solid lines) calculation results.

which indicates mixing of components and absence of a pronounced interface. In turn, the PLG solution in TG forms a stable film 20–25 Å thick on the surface. With an increase in the PLG concentration in the solution to 7 wt % one can observe a proportional increase in density, with the film structure and thickness preserved. Note that the film parameters are in agreement with the characteristic values of thickness, density, and roughness of a single sublayer, observed when depositing a solution in chloroform. The relatively low interface roughness also indicates the preferred orientation of PLG molecules being in the surface plane.

At concentrations of 5 and 10% the layer density is redistributed over depth to 50–100 Å, with preservation of the total amount of material. This fact indicates that the PLG film transits to an unstable state, in which some polymer chains "sink" into the substrate bulk. Note that this effect is reproduced at the aforementioned concentrations independently of the preparation technique and the amount of deposited solution. In addition, the estimated total roughness

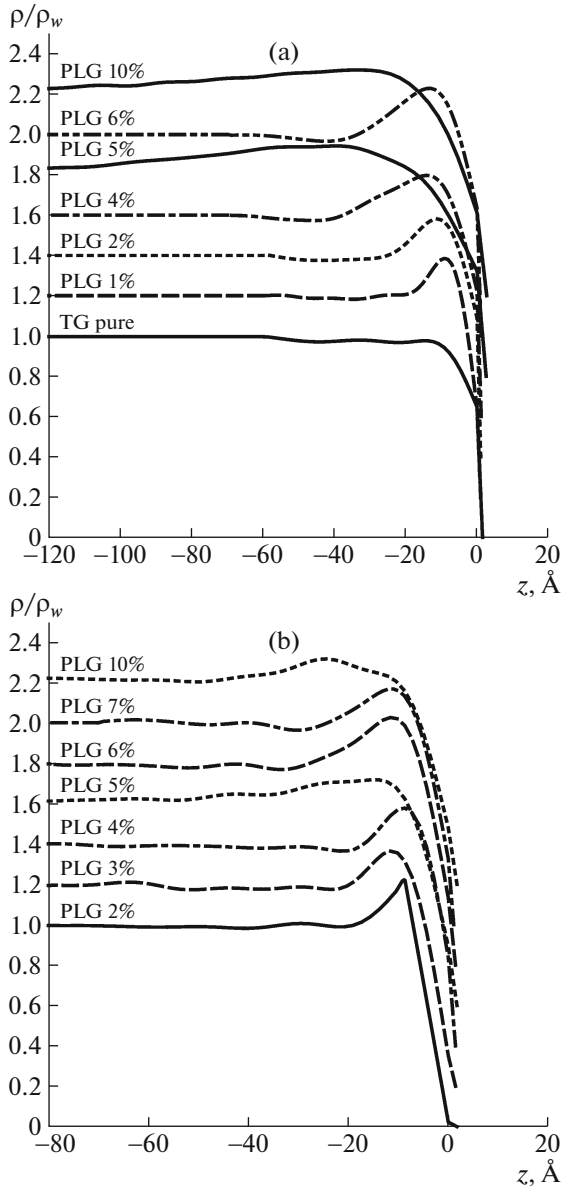

Fig. 4. Depth profiles of electron density ρ, normalized to the tabular water density $\rho_w = 0.333$ Å^{-3}, calculated for polylactoglycolide solutions in tetraglycol, prepared (a) by the method of successive dilutions and (b) based on the weight ratio.

height for the external film interface at the aforementioned concentrations increases from ~2.7 to ~4.5 Å, which indicates the existence of an additional roughness component, related presumably to the violation of packing homogeneity of polymer chains in the surface plane.

Thus, it was found that, in the entire concentration range under study, PLG solutions in chloroform and TG form a stable two-layer film on the water surface, in which polymer chains are packed relatively homogeneously along the substrate surface. The density profiles indicate the presence of a pronounced interface between the polymer phase and water, which is in agreement with the hydrophobic nature of PLG. A more thorough analysis of the structure and nature of the "folded" sublayer is an object of a separate study.

The PLG/TG/water ternary system exhibits a singularity near the concentration value of 5 wt % PLG, in which the film exists in an unstable state, changing from a planar structure with a single-layer packing of polymer chains to a diffuse layer with a partial penetration of polymer into the water substrate bulk. This can be explained by the formation of a relatively stable solvate shell from the solvent (thermodynamically compatible with water) around hydrophobic PLG macromolecules; this shell provides transport of hydrophobic macromolecules to water. The threshold type of the concentration dependence of the distribution of macromolecules in the surface layer may be related to the critical ratio of macromolecule–solvent interactions in comparison with the macromolecule–macromolecule interactions in the initial solution, below which the transport of an individual macromolecule jointly with the TG diffusing into water becomes unlikely. At the same time it was found that during the formation of a solid structure further mass exchange between the polymer solution and antisolvent occurs through a continuous hydrophobic layer up to 25 Å thick, which impedes the antisolvent diffusion into the solution. At the same time, according to the results obtained and the data of [17], this diffusion cannot be excluded completely.

FUNDING

This study was supported by the Ministry of Science and Higher Education of the Russian Federation within the State assignment for the Federal Scientific Research Centre "Crystallography and Photonics" of the Russian Academy of Sciences and for the Kapitza Institute for Physical Problems, Russian Academy of Sciences. The theoretical part of the study was supported by the Russian Foundation for Basic Research, project no. 19-29-12045.

CONFLICT OF INTEREST

The authors declare that they have no conflicts of interest.

REFERENCES

1. M. Martina and D. W. Hutmacher, Polymer Int. **56** (2), 145 (2007). https://doi.org/10.1002/pi.2108
2. A. Sensini, C. Gualandi, M. L. Focarete, et al., Biofabrication **11** (3), 035026 (2019).
3. V. Karageorgiou and D. Kaplan, Biomaterials **26** (27), 5474 (2005). https://doi.org/10.1016/j.biomaterials.2005.02.002

4. A. Pryadko, M. Surmeneva, and R. Surmenev, Polymers **13** (11), 1738 (2021). https://doi.org/10.3390/polym13111738
5. G. Q. Chen and Q. Wu, Biomaterials **26** (33), 6565 (2005). https://doi.org/10.1016/j.biomaterials.2005.04.036
6. A. Eltom, G. Zhong, and A. Muhammad, Adv. Mater. Sci. Eng. **2019**, 3429527 (2019). https://doi.org/10.1155/2019/3429527
7. H. M. Yin, J. Qian, J. Zhang, et al., Polymers **8** (6), 213 (2016). https://doi.org/10.3390/polym8060213
8. M. Adamkiewicz and B. Rubinsky, Cryobiology **71** (3), 518 (2015). https://doi.org/10.1016/j.cryobiol.2015.10.152
9. A. Kamali and A. Shamloo, J. Biomech. **98**, 109466 (2019). https://doi.org/10.1016/j.jbiomech.2019.109466
10. Z. L. Mou, L. J. Zhao, Q. A. Zhang, et al., J. Supercrit. Fluids **58**, 398 (2011). https://doi.org/10.1016/j.supflu.2011.07.003
11. H. Sun, Q. Zhao, L. W. Zheng, et al., Nano LIFE **11** (4), 2141005 (2021). https://doi.org/10.1142/S1793984421410051
12. Z. Li, Z. Jiang, L. Zhao, et al., Mater. Sci. Eng. C **81**, 443 (2017). https://doi.org/10.1016/j.msec.2017.08.019
13. P. van de Vitte, H. Esselbrugge, P. J. Dijkstra, et al., J. Membr. Sci. **113** (2), 223 (1996). https://doi.org/10.1016/0376-7388(95)00068-2
14. H. Sawalha, K. Schroen, and R. Boom, J. Appl. Polym. Sci. **104**, 959 (2007). https://doi.org/10.1002/app.25808
15. D. M. Mitrinovic, A. M. Tikhonov, M. Li, et al., Phys. Rev. Lett. **85**, 582 (2000). https://doi.org/10.1103/PhysRevLett.85.582
16. A. M. Tikhonov and M. L. Schlossman, J. Phys. Chem. B. **107**, 3344 (2003). https://doi.org/10.1021/jp0271817
17. A. V. Mironov, O. A. Mironova, M. A. Syachina, and V. K. Popov, Polymer **182** (2), 121845 (2019). https://doi.org/10.1016/j.polymer.2019.121845
18. T. Ramos and L. Moroni, Tissue Eng. Pt C: Methods **26** (2), 91 (2019). https://doi.org/10.1089/ten.tec.2019.0344
19. K. Hoshi, Y. Fujihara, T. Yamawaki, et al., Histochem. Cell. Biol. **149**, 375 (2018). https://doi.org/10.1007/s00418-018-1652-2
20. A. Aubert-Pouëssel, M. C. Venier-Julienne, P. Saulnier, et al., Pharm. Res. **21** (12), 2384 (2005). https://doi.org/10.1007/s11095-004-7693-3
21. I. W. Hamley and J. S. Pedersen, J. Appl. Cryst. **27**, 29 (1994). https://doi.org/10.1107/S0021889893006260
22. M. Tolan, *X-ray Scattering from Soft-Matter Thin Films,* Vol. 148 of *Springer Tracts in Modern Physics* (Springer, Berlin, 1999).
23. I. V. Kozhevnikov, Nucl. Instrum. Methods Phys. Res. A. **508**, 519 (2003). https://doi.org/10.1016/S0168-9002(03)01512-2
24. A. M. Tikhonov, V. E. Asadchikov, Yu. O. Volkov, et al., Prib. Tekh. Eksp., No. 1, 146 (2021). https://doi.org/10.31857/S0032816221010158
25. V. E. Asadchikov, V. G. Babak, A. V. Buzmakov, et al., Prib. Tekh. Eksp., No. 3, 99 (2005). https://doi.org/10.1007/s10786-005-0064-4
26. V. E. Asadchikov, Yu. O. Volkov, B. S. Roshchin, et al., Radioelektron. Nanosist. Inf. Tekhnol. **12** (1), 145 (2020). https://doi.org/10.17725/rensit.2020.12.145
27. I. V. Kozhevnikov, L. Peverini, and E. Ziegler, Phys. Rev. B **85**, 125439 (2012). https://doi.org/10.1103/PhysRevB.85.125439
28. A. Braslau, P. S. Pershan, J. Swislow, et al., Phys. Rev. A **38** (5), 2457 (1988). https://doi.org/10.1103/PhysRevA.38.2457

Translated by Yu. Sin'kov